

# Journal of Visualized Experiments

## Intramucosal Inoculation of Squamous Cell Carcinoma Cells in Mice for Tumor Immune Profiling and Treatment Response Assessment --Manuscript Draft--

<b>Article Type:</b>	Methods Article - JoVE Produced Video
<b>Manuscript Number:</b>	JoVE59195R2
<b>Full Title:</b>	Intramucosal Inoculation of Squamous Cell Carcinoma Cells in Mice for Tumor Immune Profiling and Treatment Response Assessment
<b>Keywords:</b>	head and neck cancer tumor microenvironment tumor immunology orthotopic tumor model mass cytometry tumor digestion
<b>Corresponding Author:</b>	Ayman J Oweida, PhD University of Colorado Denver - Anschutz Medical Campus Aurora, COLORADO UNITED STATES
<b>Corresponding Author's Institution:</b>	University of Colorado Denver - Anschutz Medical Campus
<b>Corresponding Author E-Mail:</b>	ayman.oweida@ucdenver.edu
<b>Order of Authors:</b>	Ayman J Oweida, PhD Shilpa Bhatia Laurel Darragh Natalie Serkova Sana D. Karam
<b>Additional Information:</b>	
<b>Question</b>	<b>Response</b>
Please indicate whether this article will be Standard Access or Open Access.	Standard Access (US\$2,400)
Please indicate the <b>city, state/province, and country</b> where this article will be <b>filmed</b> . Please do not use abbreviations.	Aurora, Colorado, United States

**TITLE:**

Intramucosal Inoculation of Squamous Cell Carcinoma Cells in Mice for Tumor Immune Profiling and Treatment Response Assessment

**AUTHORS AND AFFILIATIONS:**

Ayman J. Oweida<sup>1</sup>, Shilpa Bhatia<sup>1</sup>, Benjamin Van Court<sup>1</sup>, Laurel Darragh<sup>1</sup>, Natalie Serkova<sup>1,2,3</sup>, Sana D. Karam<sup>1</sup>

<sup>1</sup>Department of Radiation Oncology, University of Colorado Denver – Anschutz Medical Campus, Aurora, CO, USA

<sup>2</sup>Department of Anesthesiology, University of Colorado Denver – Anschutz Medical Campus, Aurora, Co, USA

<sup>3</sup>Division of Radiology, University of Colorado Denver – Anschutz Medical Campus, Aurora, CO, USA

Email addresses of co-authors:

Shilpa Bhatia	(Shilpa.bhatia@ucdenver.edu)
Benjamin Van Court	(Benjamin.vancourt@ucdenver.edu)
Laurel Darragh	(Laurel.darragh@ucdenver.edu)
Natalie Serkova	(Natalie.serkova@ucdenver.edu)
Sana D. Karam	(Sana.karam@ucdenver.edu)

Corresponding author:

Sana D. Karam (Sana.karam@ucdenver.edu)

**KEYWORDS:**

Head and neck cancer, orthotopic model, tumor microenvironment, immune evasion, flow cytometry, mass cytometry

**SUMMARY:**

Here we present a reproducible method for developing an orthotopic murine model of head and neck squamous cell carcinoma. Tumors demonstrate clinically relevant histopathological features of the disease, including necrosis, poor differentiation, nodal metastases, and immune infiltration. Tumor-bearing mice develop clinically relevant symptoms including dysphagia, jaw displacement, and weight loss.

**ABSTRACT:**

Head and neck squamous cell carcinoma (HNSCC) is a debilitating and deadly disease with a high prevalence of recurrence and treatment failure. To develop better therapeutic strategies, understanding tumor microenvironmental factors that contribute to the treatment resistance is important. A major impediment to understanding disease mechanisms and improving therapy has been a lack of murine cell lines that resemble the aggressive and metastatic nature of human HNSCCs. Furthermore, a majority of murine models employ subcutaneous implantations of

tumors which lack important physiological features of the head and neck region, including high vascular density, extensive lymphatic vasculature, and resident mucosal flora. The purpose of this study is to develop and characterize an orthotopic model of HNSCC. We employ two genetically distinct murine cell lines and established tumors in the buccal mucosa of mice. We optimize collagenase-based tumor digestion methods for the optimal recovery of single cells from established tumors. The data presented here show that mice develop highly vascularized tumors that metastasize to regional lymph nodes. Single-cell multiparametric mass cytometry analysis shows the presence of diverse immune populations with myeloid cells representing the majority of all immune cells. The model proposed in this study has applications in cancer biology, tumor immunology, and preclinical development of novel therapeutics. The resemblance of the orthotopic model to clinical features of human disease will provide a tool for enhanced translation and improved patient outcomes.

## INTRODUCTION:

HNSCC is the fifth most common malignancy globally, with over 600,000 patients diagnosed annually<sup>1</sup>. Despite aggressive treatment involving chemotherapy and radiotherapy (RT), the overall survival (OS) rate for HNSCC patients without human papillomavirus (HPV) infection remains below 50% after 5 years<sup>2</sup>. This is largely attributed to a highly complex tumor microenvironment as tumors can originate from several distinct anatomical sites within the head and neck region, including the buccal mucosa, tongue, floor of the mouth, nasal cavity, oral cavity, pharynx, oropharynx, and hypopharynx. In addition, the head and neck region is highly vascularized and contains nearly half of all lymph nodes in the body<sup>3</sup>. A majority of studies investigating head and neck tumor biology rely on tumor models in the flank region. Such models can offer insight into tumor-intrinsic mechanisms, but the lack of the native head and neck microenvironment can significantly impact the translational potential of such findings. One method that has been used to induce oral tumors is through exposure to the carcinogen 9,10-dimethyl-1,2-benzanthracene (DMBA)<sup>4</sup>. However, this method is associated with a lengthy process, induces tumors in rats and hamsters but not in mice, and the resulting tumors do not possess many of the histological features of differentiated SCCs<sup>5,6</sup>. The introduction of the carcinogen 4-nitroquinoline 1-oxide (4-NQO), a water-soluble quinolone derivative, resulted in mouse oral tumors when applied orally but also suffered from long exposure times (16 weeks) and a limited take rate within and between batches of mice<sup>7-9</sup>. In order to develop clinically relevant models, several groups utilized genetically engineered models involving the manipulation of driver oncogenes or tumor suppressor genes, including TP53, TGFB, KRAS, HRAS, and SMAD4<sup>10</sup>. These models can offer insight into tumors with known driver genes but do not recapitulate the complex heterogeneity of human HNSCCs.

In this work, we demonstrate the feasibility of performing an intramucosal inoculation of squamous cell carcinoma cells in mice. Inoculated cells develop into aggressive tumors within 1 week of injection. Similar to human HNSCCs, the tumors metastasize to the regional lymph nodes. We characterize histological and clinical features of the disease and provide insight into the tumor immune microenvironment. We propose that this orthotopic model of HNSCC has applications in cancer biology, tumor immunology, and preclinical studies. Mechanisms of immune evasion, tumor progression, treatment resistance, and metastases represent areas of

clinical significance that can be addressed using the proposed model.

## **PROTOCOL:**

All animal procedures were performed in accordance with an approved institutional animal care and use committee (IACUC) protocol of the University of Colorado Denver (protocol # 00250).

### **1. Tumor cell culture**

NOTE: B4B8 and LY2 cell lines were used to generate orthotopic HNSCC tumors: B4B8 tumor cells were derived from carcinogen-transformed mucosal keratinocytes (from BALB/C mice)<sup>11</sup>. LY2 tumor cells were derived from lymph node metastases of a spontaneously transformed BALB/C keratinocyte line (Pam 212)<sup>12,13</sup>. Both cell lines were kindly provided by Dr. Nadarajah Vigneswaran (UTHealth, Houston, TX, USA).

1.1. Use Dulbecco's modified Eagle's medium (DMEM) F/12 supplemented with 10% fetal bovine serum (FBS) and 1% antimicrobial reagent for the cell line maintenance. Maintain these cell lines in a sterile incubator at 37 °C and 5% CO<sub>2</sub>. Cells should be used for inoculation before exceeding 15 passages.

1.2. Plate 2 x 10<sup>6</sup> to 4 x 10<sup>6</sup> cells in 175 cm<sup>2</sup> cell culture flasks.

NOTE: Ensure the cells are less than 90% confluent to avoid inducing a stress response.

1.3. When the cells are 70% confluent (~48 h), remove the flask from the incubator and wash the cells 3x with cold phosphate-buffered saline (PBS).

1.4. Detach the cells from the flask using 0.25% trypsin, enough to cover the surface of the plate.

1.4.1. To do this, dispense 4 mL of trypsin in a 175 cm<sup>2</sup> flask containing 70% confluent cells. Incubate the cells with trypsin for 3–4 min in the cell culture incubator at 37 °C and 5% CO<sub>2</sub>.

1.4.2. Visualize the cells under a microscope to ensure cell detachment.

1.4.3. Add 12 mL of DMEM F/12 media containing FBS to neutralize trypsin activity.

1.5. Aspirate the cell suspension and place it into a 50 mL conical tube.

1.6. Shake the tube containing the cells by inverting it 3x–4x.

1.7. Optionally, mix a 10 µL aliquot of cell suspension with 10 µL of Trypan blue in a microcentrifuge tube and count the cells using a hemocytometer. Determine cell viability by subtracting the number of Trypan-blue-positive cells from the total number of cells and divide by the total number of cells.

1.8. Centrifuge the cell suspension at 300 x *g* for 5 min at 4 °C.

1.9. Resuspend the cells in serum-free and antibiotic-free DMEM at an appropriate volume so that 1 x 10<sup>6</sup> cells are present in 50 µL of media.

NOTE: Based on the in vivo cell line aggressiveness (determined empirically), 1 x 10<sup>6</sup> cells per injection site per mouse was deemed appropriate for B4B8 and LY2 cells.

1.10. Place the vial containing the cell suspension on ice.

1.11. Place the pre-thawed basement membrane matrix on ice.

NOTE: The basement membrane matrix was thawed overnight at 4 °C.

## 2. Cell injection into mice

2.1. Prepare a 1:1 mixture of cells:basement membrane matrix (50 µL each).

2.2. Add the cells first; then, gradually pipette the basement membrane matrix. Avoid introducing air bubbles. Ensure that the mixture is made immediately before the animal injection. Adding cells to basement membrane matrix for an extended period of time can result in cell settling in the matrix mixture, which makes the mixture difficult to shake rigorously. This will cause a considerable variability in tumor size between mice.

2.3. Mix gently. Ensure all steps involving matrix are performed on ice. Basement membrane matrix will polymerize at room temperature.

2.4. Prepare syringes for inoculation.

2.5. Load 0.5 mL insulin syringes (23 G) with 100 µL of the cell/basement membrane matrix solution.

2.6. Keep the syringes on ice to avoid basement membrane matrix polymerization.

2.7. Anesthetize mice by placing them in a chamber with isoflurane and oxygen (2.5%).

2.8. Ensure the mice are deeply anesthetized before performing the injection (by ensuring a lack of response to a toe pinch).

2.9. Insert the needle into the right or left buccal region. This is performed through the available open space on either side of the mouth.

2.10. Ensure that the mouse's tongue is not in the way.

NOTE: It is easy to poke the tongue, which will result in tongue tumors. Move the tongue to the opposite side if necessary.

2.11. Keep the syringe parallel to the buccal region while inside the oral cavity.

2.12. When ready to inject, pull the syringe back and slowly insert the syringe at a 10° angle.

2.13. Inject 100 µL of the cell/basement membrane matrix suspension over a period of 5 s.

2.14. Hold the syringe in place for an additional 5 s to ensure all material is injected.

NOTE: For control nontumor-bearing mice, inject a mixture of serum-free media and matrix (as described above) without the tumor cells.

2.15. Withdraw the syringe gently.

2.16. Continue the above procedure with the remaining mice.

2.17. Allow for 1 week until tumors begin to appear grossly (50–200 mm<sup>3</sup> for B4B8 and LY2 cells).

### 3. Mouse monitoring

3.1. Perform the first measurement using calipers at 1 week after the tumor cell injection. In order to calculate the tumor volume using external calipers, determine the greatest longitudinal diameter (length) and the greatest transverse diameter (width) and use the modified ellipsoidal formula<sup>14,15</sup>.

$$\text{Tumor volume} = \frac{1}{2}(\text{length} \times \text{width}^2)$$

3.2. Continue to perform regular caliper measurements for tumor volume (1x–2x per week at regular intervals).

3.3. Measure animal weight to assess the effects of tumor growth on feeding.

### 4. Harvesting tumors

4.1. When the experimental endpoint is reached, euthanize the animals using appropriate measures (e.g., CO<sub>2</sub> asphyxiation, decapitation, or cervical dislocation).

NOTE: In this study, the endpoint was reached if the mice became moribund (with a weight loss of >15% of their initial weight, a lack of grooming, cachexia) and/or if the tumor size reached 1,000 mm<sup>3</sup>.

220 4.2. Begin dissecting the animal by creating a long incision through the midline in the neck region.

221  
222 4.2.1. Use blunt forceps to grab the skin and sharp scissors to cut the skin.

223  
224 4.3. Insert scissors gently under the skin covering the tumor and create air pockets by pushing  
225 the scissors across and into the skin.

226  
227 4.4. Once the skin is sufficiently detached from the tumor, identify the draining lymph nodes  
228 (DLNs) and excise them to avoid having the tumor tissue confounded by the presence of lymph  
229 nodes.

230  
231 NOTE: Large tumors may reach and/or cover the DLN. Depending on the type of assay being  
232 performed, the isolation of intact lymph nodes is essential to avoid spillage of immune cells into  
233 the tumor, which will result in skewing the assay results.

234  
235 4.5. Cut through the borders of the tumor until the entire volume is detached.

## 236 237 5. Tumor processing for downstream applications

238  
239 5.1. For the downstream histologic examination, place tumors in 10% formalin at room  
240 temperature. To avoid overfixation, replace the formalin with 70% ethanol. For flow cytometry  
241 analysis, process the tumors as described below.

242  
243 NOTE: The tissue can be kept in formalin for 72 h before overfixation can become problematic  
244 for certain types of staining.

245  
246 5.2. Cut the tumor into 1–2 mm-sized pieces using a sterile razor blade or sharp scissors.

247  
248 5.3. Place the cut tumor pieces in a 50 mL conical tube with collagenase III (4,250 units per  
249 sample), DNase I (0.1 mg per sample), and trypsin inhibitor (1 mg per sample).

250  
251 5.4. Incubate at 37 °C for 30 min with shaking every 10 min.

252  
253 NOTE: The samples can be placed in a resealable bag, sterilized with 90% ethanol, and placed in  
254 a cell culture incubator.

255  
256 5.5. After 30 min, add 20 mL of Hank's balanced salt solution (HBSS) and spin at 300 x g for 5 min.

257  
258 NOTE: HBSS is comprised of potassium chloride, sodium chloride, sodium bicarbonate, sodium  
259 phosphate dibasic, sodium phosphate monobasic and glucose.

260  
261 5.6. Discard the supernatant and resuspend the pellet in 2–3 mL of red blood cell (RBC) lysis  
262 buffer. Pipette rigorously.

NOTE: RBC lysis buffer is comprised of ammonium chloride, sodium bicarbonate, and disodium.

**5.7. Incubate for 2 min at room temperature.**

NOTE: Longer incubation can be toxic to other cell populations.

**5.8. Add 20 mL of HBSS to neutralize the effect of lysis buffer.**

**5.9. Centrifuge at 300 x *g* for 5 min and discard the supernatant.**

**5.10. Resuspend the pellet in 10 mL of HBSS.**

**5.11. Pass the solution through a 70 µm nylon restrainer and centrifuge at 300 x *g* for 5 min. Discard the supernatant.**

**5.12. Repeat steps 5.8–5.10 and pass the cell suspension through a 40 µm nylon restrainer to ensure any additional debris is removed from the suspension.**

**6. Cell staining and data acquisition**

6.1. Resuspend the cell pellet in 1 mL of HBSS.

6.2. Count the cells using a hemocytometer or an automated cell counter, as described in step 1.7

6.3. Determine the total cell number and appropriate concentration for staining.

NOTE: The ideal cell concentration for flow cytometry staining is 1–2 million cells. For example, if staining is performed in a 96-well plate and there are 10 million cells, resuspend the sample in 1 mL and plate 100 µL for 1 million cells per well.

6.4. Add Fc block (CD16/CD32) at a concentration of 1:100 in order to prevent nonantigen-specific binding of immunoglobulins to the FcγIII and FcγII receptors. Incubate for 5 min at room temperature.

6.4.1. Centrifuge and resuspend the cell pellet in 100 µL of flow cytometry cell staining buffer (comprised of saline solution containing 5% FBS, 2% EDTA, and 1% HEPES).

6.5. Perform cell surface staining according to supplier-provided instructions (adding each antibody at the appropriate dilution). Incubate for 60 min at room temperature.

6.5.1. Centrifuge and resuspend the cell pellet in 100 µL of HBSS. Repeat 2x to get rid of excess antibody.



6.6. Run samples on an appropriate flow cytometer.

6.6.1. If analyzing intracellular markers (e.g., foxp3), perform cell permeabilization and staining according to the supplier's instructions.

### REPRESENTATIVE RESULTS:

The in vitro assessment of LY2 and B4B8 cell proliferation showed that both cell lines have similar doubling times (21 h and 23 h, respectively). In vivo, both cell lines formed a single, visible, and palpable mass within 1 week of inoculation (**Figure 1A**). In mice bearing LY2 tumors, the jaw was displaced by 3 weeks due to tumor burden (**Figure 1A**). Control mice that did not receive tumor cells did not develop tumors as anticipated. LY2 tumors grew at a higher rate compared to B4B8 tumors. The average tumor volume on day 21 in LY2 tumor-bearing mice was  $632 \pm 10 \text{ mm}^3$  compared to  $162 \pm 4 \text{ mm}^3$  in B4B8 tumors (**Figure 1B**). Mice exhibiting jaw displacement rapidly developed weight loss due to dysphagia (**Figure 1C**). Mice exhibiting significant weight loss defined as >15% of their initial weight and/or having a tumor volume of >1 cm<sup>3</sup> were euthanized within 1 day of the noted observation. The median survival in LY2 mice was 22.5 days, compared to 52.0 days in B4B8 tumor-bearing mice (**Figure 1D**).

Magnetic resonance imaging (MRI) of tumor-bearing mice showed well-demarcated tumors extending into the inner layer of the buccal mucosa (**Figure 2A**). Tumors did not invade into the tongue or other nearby organs (esophagus, bronchus, thymus) as shown with histological assessment. Signal heterogeneity on MR images was representative of the presence of vascularized hyperintense regions (denoted with V) and necrotic hypointense regions (denoted with N) (**Figure 2A**). A gross pathological examination showed enlarged DLNs (**Figure 2B**). We further assessed tumor volume with computed tomography (CT) to determine the reliability of the caliper measurements. Tumors were delineated using a digital imaging and communications in medicine (DICOM) image analysis software<sup>16</sup>. Assessment of LY2 tumor volume by calipers and CT imaging showed an excellent correlation between the two methods ( $R^2 = 0.8493$ ; **Figure 2C**). This indicates that tumor growth is primarily exophytic and caliper measurement is a reliable method for the assessment of tumor growth. Histologic examination showed that all LY2 tumor-bearing mice developed poorly differentiated squamous cell carcinoma (**Figure 2D**). Nine out of nine LY2 tumor-bearing mice developed metastases to the first and second echelon lymph nodes. Nodal metastases were primarily subcapsular (with seven out of nine mice) and within sinuses (with five out of nine mice), with two out of nine mice demonstrating intracapsular invasion. In contrast, mice bearing B4B8 tumors developed moderately differentiated squamous cell carcinoma (**Figure 2E**) and did not metastasize to regional or distant sites, including DLNs. Necrosis was assessed based on a previously established three-grade scale: 0 = no visible necrosis, 1 = scant, 2 = moderate, and 3 = severe<sup>17</sup>. All LY2 tumor-bearing mice had histologically confirmed necrosis with the majority (seven out of ten) demonstrating moderate to severe necrosis (**Figure 2F**). No evidence of necrosis was observed in B4B8 tumors.

We focused on the LY2 tumor model for further characterization of the tumor-immune microenvironment. Tumors were harvested at 3 weeks after the tumor inoculation and digested using collagenase III, followed by the staining of the cell surface and intracellular markers for

flow/mass cytometry (**Figure 3A**). Samples were processed, using a mass cytometer, at the University of Colorado Denver Flow Cytometry Shared Resource. Gating and data analysis were performed using flow cytometry commercial software. The data obtained showed the presence of numerous immune cell populations to varying degrees. Total immune cells (CD45+) represented 7.3% of the total tumor (**Figure 3B**). In absolute numbers, we observed, on average, 26 CD45+ cells (SD = 0.81) per milligram of tumor tissue (**Figure 3B**). Myeloid cells (CD11b+) represented 37.8% of all CD45+ cells (**Figure 3C**). Myeloid cells were largely comprised of macrophages (F4/80+, 63.0%), followed by myeloid-derived suppressor cells (MDSCs) (Gr1+, 8.51%) and neutrophils (Ly6G+, 5.87%). Total T cells comprised 15.9% of CD45+ cells with CD4+ T cells comprising the majority of all T cells (79.4%), of which 53.4% were regulatory T cells (Tregs) (CD4+FoxP3+) (**Figure 3D**). Natural killer (NK) cells comprised 1.75% of all CD45+ cells. These data highlight the presence of various immune infiltrates in LY2 orthotopic HNSCC tumors which likely play a role in mediating tumor progression and immune evasion.

#### FIGURE AND TABLE LEGENDS:

**Figure 1: Monitoring mice bearing orthotopic HNSCC tumors.** (A) Representative images of tumor-bearing mice. The inoculated buccal develops a tumor within 1 week of inoculation. At 3 weeks, displacement of the jaw is observed. (B) Tumor growth rate in B4B8 and LY2 tumor-bearing mice as determined by caliper measurements. (C) Changes in the body weight of mice bearing B4B8 or LY2 tumors. (D) Survival of B4B8 and LY2 tumor-bearing mice. The bars represent the standard error of the mean (SEM) of 7–10 mice per group.

**Figure 2: Imaging and histologic features of murine HNSCC tumors.** (A) Representative coronal MR image of an LY2 tumor-bearing mouse. Anatomic sites are labeled. Areas of signal hyperintensity represent vascularized regions (denoted V). Regions of signal hypointensity represent necrotic areas (denote N). (B) Representative gross image of a dissected tumor-containing region. White arrows point to enlarged draining lymph nodes (DLNs). (C) Correlation of tumor volume as assessed by caliper measurement versus computed tomography (CT)-based assessment. Slope, correlation coefficient ( $R^2$ ), and line of best fit are shown. (D) Representative hematoxylin and eosin (H&E) image of LY2 tumor. (E) Representative H&E image of B4B8 tumor. (F) Quantification of necrosis in LY2 tumors, based on an H&E four-grade scoring system.

**Figure 3: Analysis of baseline intratumoral immune populations using cytometry by time-of-flight (CyTOF).** Tumors were processed into a single-cell suspension using collagenase-based enzymatic digestion and, then, stained with cell surface and intracellular markers. (A) Mass cytometry was performed using the CyTOF platform. (B) Absolute and relative quantitative assessment of total immune cells (CD45+). (C) Quantification of myeloid-immune subpopulations. (D) Quantification of lymphoid immune subpopulations.

#### DISCUSSION:

Rigorous analysis and characterization of the tumor microenvironment represent an important strategy for understanding mechanisms of tumor development, progression, and metastases and for the development of effective therapies. Head and neck cancer is a complex disease that can

originate from multiple anatomical sites within the head and neck region. A major impediment to understanding disease mechanisms and improving therapy has been a lack of murine mouse cell lines that resemble the aggressive and metastatic nature of human HNSCCs. Furthermore, numerous murine models employ a subcutaneous implantation of tumors which lack important physiological features of the head and neck region, including a high vascular density, an extensive lymphatic vasculature, and resident mucosal flora.

In this study, we characterized an orthotopic model of murine HNSCC. We chose the buccal mucosa as the site of tumor inoculation for a number of reasons, including easy access to the region without the need for image guidance, the ability to assess tumor growth using calipers, the presence of the tumor within the mucosal flora, the presence of surrounding lymphatics, and the ease of reproducibility. Although the injection of cells into the buccal mucosa is straightforward, the positioning of the needle and the depth of penetration are critical to prevent puncture through the skin and ensure cells are not injected subcutaneously. We recommend inserting the needle intra-orally while it is perfectly parallel to the buccal region and tilting at an angle no greater than 10° when ready to inject.

The cell lines we used were murine cell lines allowing their implantation in immunocompetent mice of the strain they were derived from. There are over 39 HNSCC human cell lines that have been studied in the literature but cannot be used in the presence of a native microenvironment<sup>18</sup>. Recent developments allowed for the design of humanized mouse models which integrate human bone-marrow-derived chimeras in NOD scid gamma mice (also known as NSG mice), allowing the development of a human immune system that can interact with human tumors in an immunodeficient mouse model<sup>19</sup>. However, such models are costly, require laborious breeding methods, and do not recapitulate all the components of the tumor microenvironment, including endothelial cells, fibroblasts, and lymphatics. The murine mouse models we employed in this study recapitulate critical components of human HNSCCs, including the presence of various immune infiltrates. To ensure maximum retrieval of viable single cells from tumors, the use of digestion enzymes is necessary. Collagenase-based digestion enzymes can be harsh on cells and the optimization of the concentration and type of collagenase may be necessary for different tumor types. We compared five digestion enzymes before determining that collagenase III, which was used in this study, is the optimal method for digestion of squamous cell tumors.

The tumor models used in this study are particularly useful for studying mechanisms of HNSCC immune evasion and preclinical assessment of various therapies. We previously demonstrated that both B4B8 and LY2 tumors are radioresistant and refractory to the immune checkpoint inhibitor anti-PD-L1<sup>20</sup>. This is consistent with the majority of human HNSCCs. Recent clinical trials showed that less than 15% of HNSCC patients are responsive to anti-PD-1/PD-L1 therapy<sup>21-25</sup>. In addition, it is well established that HNSCCs are radioresistant<sup>26,27</sup>. Targeting pathways responsible for radioresistance in HNSCC is an important step for enhancing treatment response. The landmark Bonner et al. study showed a significant benefit in overall survival with the addition of cetuximab to RT compared to RT alone in locally advanced HNSCC patients<sup>28</sup>. Recent data demonstrate that the inhibition of EphB4-Ephrin-B2 signaling in orthotopic HNSCCs can further improve the response to RT or cetuximab-RT by promoting tumor apoptosis and inhibiting tumor

proliferation<sup>29,30</sup>. In addition, combining RT with rational immune therapies can augment antitumor immune responses and enhance both local tumor control and control of distant metastases<sup>31</sup>. We have recently demonstrated that targeting Tregs in combination with immune checkpoint blockade and RT results in tumor eradication and immunologic memory<sup>32</sup>. Future studies employing orthotopic models of HNSCC will better inform the design of clinical trials and improve the understanding of mechanisms of tumor immune evasion and treatment resistance.

#### ACKNOWLEDGMENTS

None

#### DISCLOSURES:

The authors have nothing to disclose.

#### REFERENCES:

1. Chaturvedi, A. K. et al. Worldwide trends in incidence rates for oral cavity and oropharyngeal cancers. *Journal of Clinical Oncology*. **31** (36), 4550-4559, doi:10.1200/JCO.2013.50.3870 (2013).
2. Ang, K. K., Sturgis, E. M. Human papillomavirus as a marker of the natural history and response to therapy of head and neck squamous cell carcinoma. *Seminars in Radiation Oncology*. **22** (2), 128-142, doi:10.1016/j.semradonc.2011.12.004 (2012).
3. Amin, M. B. et al. The Eighth Edition AJCC Cancer Staging Manual: Continuing to build a bridge from a population-based to a more "personalized" approach to cancer staging. *CA: A Cancer Journal for Clinicians*. **67** (2), 93-99, doi:10.3322/caac.21388 (2017).
4. Salley, J. J. Experimental carcinogenesis in the cheek pouch of the Syrian hamster. *Journal of Dental Research*. **33** (2), 253-262, doi:10.1177/00220345540330021201 (1954).
5. Morris, A. L. Factors influencing experimental carcinogenesis in the hamster cheek pouch. *Journal of Dental Research*. **40**, 3-15, doi:10.1177/00220345610400012001 (1961).
6. MacDonald, D. G. Comparison of epithelial dysplasia in hamster cheek pouch carcinogenesis and human oral mucosa. *Journal of Oral Pathology & Medicine*. **10** (3), 186-191 (1981).
7. Hawkins, B. L. et al. 4NQO carcinogenesis: a mouse model of oral cavity squamous cell carcinoma. *Head & Neck*. **16** (5), 424-432 (1994).
8. Tang, X. H., Knudsen, B., Bemis, D., Tickoo, S., Gudas, L. J. Oral cavity and esophageal carcinogenesis modeled in carcinogen-treated mice. *Clinical Cancer Research*. **10** (1 Pt 1), 301-313 (2004).
9. Vered, M., Yarom, N., Dayan, D. 4NQO oral carcinogenesis: animal models, molecular markers and future expectations. *Oral Oncology*. **41** (4), 337-339, doi:10.1016/j.oraloncology.2004.07.005 (2005).
10. Bornstein, S. et al. Smad4 loss in mice causes spontaneous head and neck cancer with increased genomic instability and inflammation. *Journal of Clinical Investigation*. **119** (11), 3408-3419, doi:10.1172/JCI38854 (2009).
11. Thomas, G. R., Chen, Z., Oechsli, M. N., Hendler, F. J., Van Waes, C. Decreased expression of CD80 is a marker for increased tumorigenicity in a new murine model of oral squamous-cell carcinoma. *International Journal of Cancer*. **82** (3), 377-384 (1999).
12. Yuspa, S. H., Hawley-Nelson, P., Koehler, B., Stanley, J. R. A survey of transformation markers in differentiating epidermal cell lines in culture. *Cancer Research*. **40** (12), 4694-4703 (1980).

13. Chen, Z., Smith, C. W., Kiel, D., Van Waes, C. Metastatic variants derived following in vivo tumor progression of an in vitro transformed squamous cell carcinoma line acquire a differential growth advantage requiring tumor-host interaction. *Clinical & Experimental Metastasis*. **15** (5), 527-537 (1997).
14. Euhus, D. M., Hudd, C., LaRegina, M. C., Johnson, F. E. Tumor measurement in the nude mouse. *Journal of Surgical Oncology*. **31** (4), 229-234 (1986).
15. Tomayko, M. M., Reynolds, C. P. Determination of subcutaneous tumor size in athymic (nude) mice. *Cancer Chemotherapy and Pharmacology*. **24** (3), 148-154 (1989).
16. Yushkevich, P. A. et al. User-guided 3D active contour segmentation of anatomical structures: significantly improved efficiency and reliability. *NeuroImage*. **31** (3), 1116-1128, doi:10.1016/j.neuroimage.2006.01.015 (2006).
17. Dutta, S. et al. The relationship between tumour necrosis, tumour proliferation, local and systemic inflammation, microvessel density and survival in patients undergoing potentially curative resection of oesophageal adenocarcinoma. *British Journal of Cancer*. **106** (4), 702-710, doi:10.1038/bjc.2011.610 (2012).
18. Li, H. et al. Genomic analysis of head and neck squamous cell carcinoma cell lines and human tumors: a rational approach to preclinical model selection. *Molecular Cancer Research*. **12** (4), 571-582, doi:10.1158/1541-7786.MCR-13-0396 (2014).
19. Walsh, N. C. et al. Humanized Mouse Models of Clinical Disease. *Annual Review of Pathology*. **12**, 187-215, doi:10.1146/annurev-pathol-052016-100332 (2017).
20. Oweida, A. et al. Ionizing radiation sensitizes tumors to PD-L1 immune checkpoint blockade in orthotopic murine head and neck squamous cell carcinoma. *Onc Immunology*. **6** (10), e1356153, doi:10.1080/2162402X.2017.1356153 (2017).
21. Ferris, R. et al. Further evaluations of nivolumab (nivo) versus investigator's choice (IC) chemotherapy for recurrent or metastatic (R/M) squamous cell carcinoma of the head and neck (SCCHN): CheckMate 141. *Journal of Clinical Oncology*. **34** (suppl; abstr 6009) (2016).
22. Ferris, R. L. et al. Nivolumab for Recurrent Squamous-Cell Carcinoma of the Head and Neck. *The New England Journal of Medicine*. **375** (19), 1856-1867, doi:10.1056/NEJMoa1602252 (2016).
23. Harrington, K. J. et al. Nivolumab versus standard, single-agent therapy of investigator's choice in recurrent or metastatic squamous cell carcinoma of the head and neck (CheckMate 141): health-related quality-of-life results from a randomised, phase 3 trial. *The Lancet Oncology*. **18** (8), 1104-1115, doi:10.1016/S1470-2045(17)30421-7 (2017).
24. Kiyota, N. et al. A randomized, open-label, Phase III clinical trial of nivolumab vs. therapy of investigator's choice in recurrent squamous cell carcinoma of the head and neck: A subanalysis of Asian patients versus the global population in checkmate 141. *Oral Oncology*. **73**, 138-146, doi:10.1016/j.oraloncology.2017.07.023 (2017).
25. Ling, D. C., Bakkenist, C. J., Ferris, R. L., Clump, D. A. Role of Immunotherapy in Head and Neck Cancer. *Seminars in Radiation Oncology*. **28** (1), 12-16, doi:10.1016/j.semradonc.2017.08.009 (2018).
26. Perri, F. et al. Radioresistance in head and neck squamous cell carcinoma: Biological bases and therapeutic implications. *Head & Neck*. **37** (5), 763-770, doi:10.1002/hed.23837 (2015).
27. Yamamoto, V. N., Thylur, D. S., Bauschard, M., Schmale, I., Sinha, U. K. Overcoming radioresistance in head and neck squamous cell carcinoma. *Oral Oncology*. **63**, 44-51,

doi:10.1016/j.oraloncology.2016.11.002 (2016).

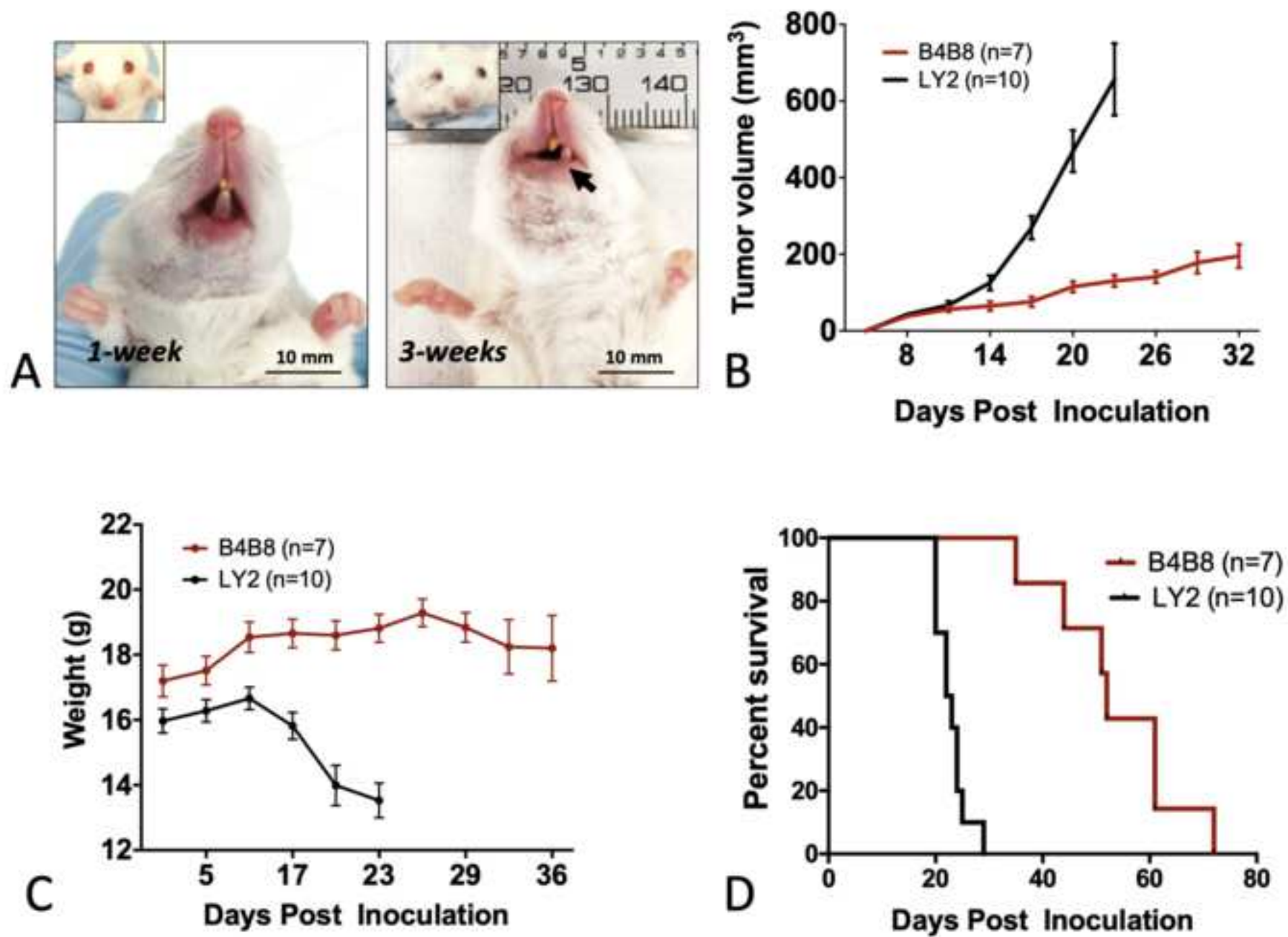
28. Bonner, J. A. et al. Radiotherapy plus cetuximab for locoregionally advanced head and neck cancer: 5-year survival data from a phase 3 randomised trial, and relation between cetuximab-induced rash and survival. *The Lancet Oncology*. **11** (1), 21-28, doi:10.1016/S1470-2045(09)70311-0 (2010).

29. Bhatia, S. et al. Inhibition of EphB4-Ephrin-B2 Signaling Enhances Response to Cetuximab-Radiation Therapy in Head and Neck Cancers. *Clinical Cancer Research*. **24** (18), 4539-4550, doi:10.1158/1078-0432.CCR-18-0327 (2018).

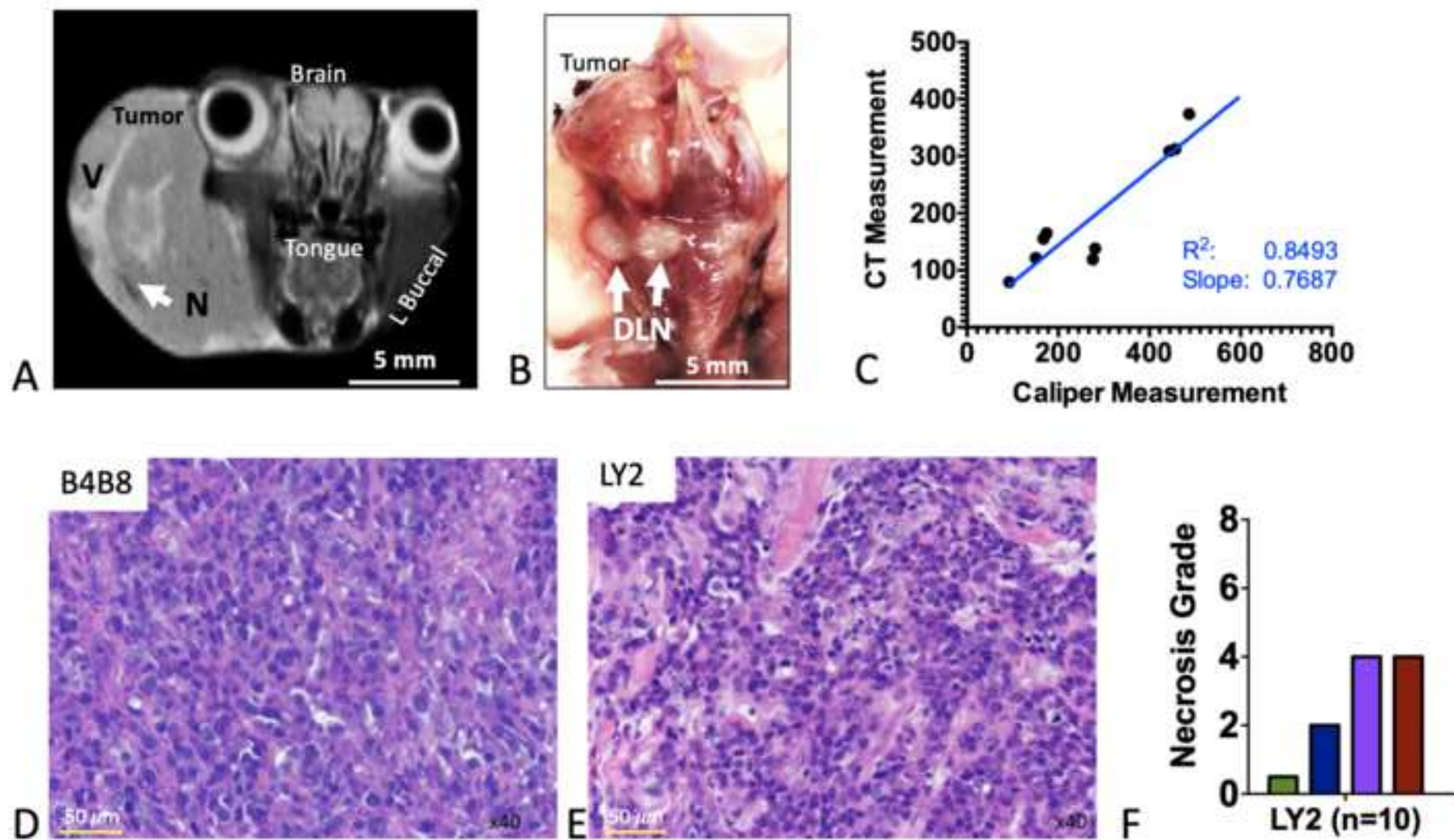
30. Bhatia, S. et al. Enhancing radiosensitization in EphB4 receptor-expressing Head and Neck Squamous Cell Carcinomas. *Scientific Reports*. **6**, 38792, doi:10.1038/srep38792 (2016).

31. Tang, C. et al. Combining radiation and immunotherapy: a new systemic therapy for solid tumors? *Cancer Immunology Research*. **2** (9), 831-838, doi:10.1158/2326-6066.CIR-14-0069 (2014).

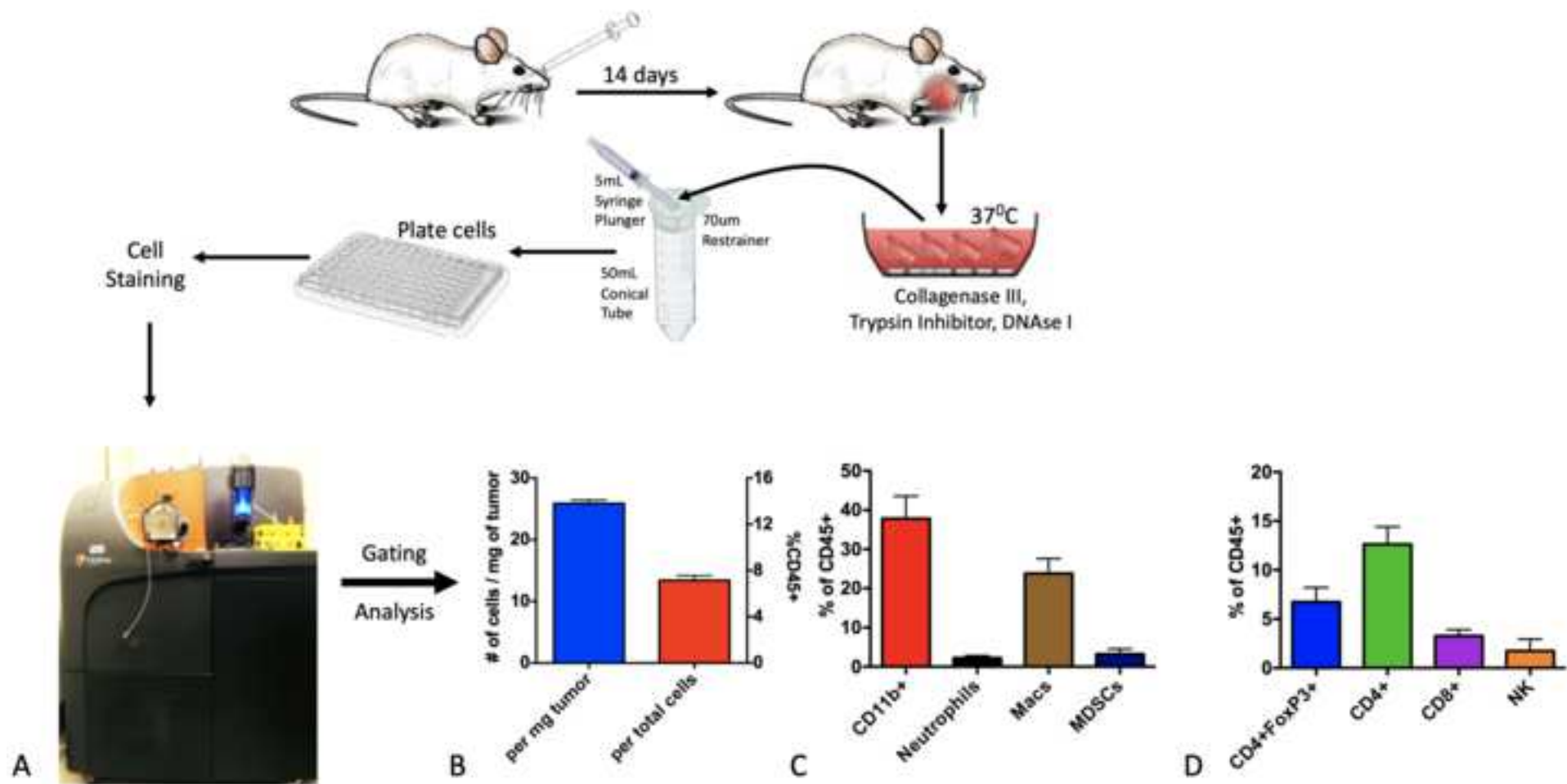
32. Oweida, A. et al. Resistance to radiotherapy and PD-L1 blockade is mediated by TIM-3 upregulation and regulatory T-cell infiltration. *Clinical Cancer Research*. doi:10.1158/1078-0432.CCR-18-1038 (2018).











<b>Name of Material/ Equipment</b>	<b>Company</b>
Collagenase III	Worthington Biochemical Corp
DNase I	Worthington Biochemical Corp
Fc Block (CD16/32)	BD Biosciences
Flow Cytometry Staining Buffer	eBioscience
HBSS	ThermoFisher Scientific
Helois mass cytometer	Fluidigm
Matrigel membrane matrix	Corning
MRI Scanner	Bruker
RBC lysis buffer	BioLegend
Trypsin inhibitor	Worthington Biochemical Corp

<b>Catalog Number</b>	<b>Comments/Description</b>
LS004183	
LS006328	
553141	Clone 2.4G2
00-4222-26	
14175079	no calcium, no magnesium, no pheno red
NA	
CB-40234B	
NA	7.4 Tesla
420301	
LS002830	

## ARTICLE AND VIDEO LICENSE AGREEMENT

Title of Article:

Development of an Orthotopic Animal Model for Recapitulation of the Native Microenvironment of Head and Neck Cancers

Author(s):

Ayman J. Oweida, Shilpa Bhatia, Laurel Darragh, Natalie Serkova, Sana D. Karam

Item 1: The Author elects to have the Materials be made available (as described at <http://www.jove.com/publish>) via:



Standard Access



Open Access

Item 2: Please select one of the following items:



The Author is **NOT** a United States government employee.



The Author is a United States government employee and the Materials were prepared in the course of his or her duties as a United States government employee.



The Author is a United States government employee but the Materials were NOT prepared in the course of his or her duties as a United States government employee.

### ARTICLE AND VIDEO LICENSE AGREEMENT

1. **Defined Terms.** As used in this Article and Video License Agreement, the following terms shall have the following meanings: “**Agreement**” means this Article and Video License Agreement; “**Article**” means the article specified on the last page of this Agreement, including any associated materials such as texts, figures, tables, artwork, abstracts, or summaries contained therein; “**Author**” means the author who is a signatory to this Agreement; “**Collective Work**” means a work, such as a periodical issue, anthology or encyclopedia, in which the Materials in their entirety in unmodified form, along with a number of other contributions, constituting separate and independent works in themselves, are assembled into a collective whole; “**CRC License**” means the Creative Commons Attribution-Non Commercial-No Derivs 3.0 Unported Agreement, the terms and conditions of which can be found at: <http://creativecommons.org/licenses/by-nc-nd/3.0/legalcode>; “**Derivative Work**” means a work based upon the Materials or upon the Materials and other pre-existing works, such as a translation, musical arrangement, dramatization, fictionalization, motion picture version, sound recording, art reproduction, abridgment, condensation, or any other form in which the Materials may be recast, transformed, or adapted; “**Institution**” means the institution, listed on the last page of this Agreement, by which the Author was employed at the time of the creation of the Materials; “**JoVE**” means MyJoVE Corporation, a Massachusetts corporation and the publisher of The Journal of Visualized Experiments; “**Materials**” means the Article and / or the Video; “**Parties**” means the Author and JoVE; “**Video**” means any video(s) made by the Author, alone or in conjunction with any other parties, or by JoVE or its affiliates or agents, individually or in collaboration with the Author or any other parties, incorporating all or any portion

of the Article, and in which the Author may or may not appear.

2. **Background.** The Author, who is the author of the Article, in order to ensure the dissemination and protection of the Article, desires to have the JoVE publish the Article and create and transmit videos based on the Article. In furtherance of such goals, the Parties desire to memorialize in this Agreement the respective rights of each Party in and to the Article and the Video.

3. **Grant of Rights in Article.** In consideration of JoVE agreeing to publish the Article, the Author hereby grants to JoVE, subject to **Sections 4** and **7** below, the exclusive, royalty-free, perpetual (for the full term of copyright in the Article, including any extensions thereto) license (a) to publish, reproduce, distribute, display and store the Article in all forms, formats and media whether now known or hereafter developed (including without limitation in print, digital and electronic form) throughout the world, (b) to translate the Article into other languages, create adaptations, summaries or extracts of the Article or other Derivative Works (including, without limitation, the Video) or Collective Works based on all or any portion of the Article and exercise all of the rights set forth in (a) above in such translations, adaptations, summaries, extracts, Derivative Works or Collective Works and (c) to license others to do any or all of the above. The foregoing rights may be exercised in all media and formats, whether now known or hereafter devised, and include the right to make such modifications as are technically necessary to exercise the rights in other media and formats. If the “Open Access” box has been checked in **Item 1** above, JoVE and the Author hereby grant to the public all such rights in the Article as provided in, but subject to all limitations and requirements set forth in, the CRC License.

## ARTICLE AND VIDEO LICENSE AGREEMENT

4. **Retention of Rights in Article.** Notwithstanding the exclusive license granted to JoVE in **Section 3** above, the Author shall, with respect to the Article, retain the non-exclusive right to use all or part of the Article for the non-commercial purpose of giving lectures, presentations or teaching classes, and to post a copy of the Article on the Institution's website or the Author's personal website, in each case provided that a link to the Article on the JoVE website is provided and notice of JoVE's copyright in the Article is included. All non-copyright intellectual property rights in and to the Article, such as patent rights, shall remain with the Author.

5. **Grant of Rights in Video – Standard Access.** This **Section 5** applies if the "Standard Access" box has been checked in **Item 1** above or if no box has been checked in **Item 1** above. In consideration of JoVE agreeing to produce, display or otherwise assist with the Video, the Author hereby acknowledges and agrees that, Subject to **Section 7** below, JoVE is and shall be the sole and exclusive owner of all rights of any nature, including, without limitation, all copyrights, in and to the Video. To the extent that, by law, the Author is deemed, now or at any time in the future, to have any rights of any nature in or to the Video, the Author hereby disclaims all such rights and transfers all such rights to JoVE.

6. **Grant of Rights in Video – Open Access.** This **Section 6** applies only if the "Open Access" box has been checked in **Item 1** above. In consideration of JoVE agreeing to produce, display or otherwise assist with the Video, the Author hereby grants to JoVE, subject to **Section 7** below, the exclusive, royalty-free, perpetual (for the full term of copyright in the Article, including any extensions thereto) license (a) to publish, reproduce, distribute, display and store the Video in all forms, formats and media whether now known or hereafter developed (including without limitation in print, digital and electronic form) throughout the world, (b) to translate the Video into other languages, create adaptations, summaries or extracts of the Video or other Derivative Works or Collective Works based on all or any portion of the Video and exercise all of the rights set forth in (a) above in such translations, adaptations, summaries, extracts, Derivative Works or Collective Works and (c) to license others to do any or all of the above. The foregoing rights may be exercised in all media and formats, whether now known or hereafter devised, and include the right to make such modifications as are technically necessary to exercise the rights in other media and formats. For any Video to which this **Section 6** is applicable, JoVE and the Author hereby grant to the public all such rights in the Video as provided in, but subject to all limitations and requirements set forth in, the CRC License.

7. **Government Employees.** If the Author is a United States government employee and the Article was prepared in the course of his or her duties as a United States government employee, as indicated in **Item 2** above, and any of the licenses or grants granted by the Author hereunder exceed the scope of the 17 U.S.C. 403, then the rights granted hereunder shall be limited to the maximum

rights permitted under such statute. In such case, all provisions contained herein that are not in conflict with such statute shall remain in full force and effect, and all provisions contained herein that do so conflict shall be deemed to be amended so as to provide to JoVE the maximum rights permissible within such statute.

8. **Protection of the Work.** The Author(s) authorize JoVE to take steps in the Author(s) name and on their behalf if JoVE believes some third party could be infringing or might infringe the copyright of either the Author's Article and/or Video.

9. **Likeness, Privacy, Personality.** The Author hereby grants JoVE the right to use the Author's name, voice, likeness, picture, photograph, image, biography and performance in any way, commercial or otherwise, in connection with the Materials and the sale, promotion and distribution thereof. The Author hereby waives any and all rights he or she may have, relating to his or her appearance in the Video or otherwise relating to the Materials, under all applicable privacy, likeness, personality or similar laws.

10. **Author Warranties.** The Author represents and warrants that the Article is original, that it has not been published, that the copyright interest is owned by the Author (or, if more than one author is listed at the beginning of this Agreement, by such authors collectively) and has not been assigned, licensed, or otherwise transferred to any other party. The Author represents and warrants that the author(s) listed at the top of this Agreement are the only authors of the Materials. If more than one author is listed at the top of this Agreement and if any such author has not entered into a separate Article and Video License Agreement with JoVE relating to the Materials, the Author represents and warrants that the Author has been authorized by each of the other such authors to execute this Agreement on his or her behalf and to bind him or her with respect to the terms of this Agreement as if each of them had been a party hereto as an Author. The Author warrants that the use, reproduction, distribution, public or private performance or display, and/or modification of all or any portion of the Materials does not and will not violate, infringe and/or misappropriate the patent, trademark, intellectual property or other rights of any third party. The Author represents and warrants that it has and will continue to comply with all government, institutional and other regulations, including, without limitation all institutional, laboratory, hospital, ethical, human and animal treatment, privacy, and all other rules, regulations, laws, procedures or guidelines, applicable to the Materials, and that all research involving human and animal subjects has been approved by the Author's relevant institutional review board.

11. **JoVE Discretion.** If the Author requests the assistance of JoVE in producing the Video in the Author's facility, the Author shall ensure that the presence of JoVE employees, agents or independent contractors is in accordance with the relevant regulations of the Author's institution. If more than one author is listed at the beginning of this Agreement, JoVE may, in its sole

## ARTICLE AND VIDEO LICENSE AGREEMENT

discretion, elect not take any action with respect to the Article until such time as it has received complete, executed Article and Video License Agreements from each such author. JoVE reserves the right, in its absolute and sole discretion and without giving any reason therefore, to accept or decline any work submitted to JoVE. JoVE and its employees, agents and independent contractors shall have full, unfettered access to the facilities of the Author or of the Author's institution as necessary to make the Video, whether actually published or not. JoVE has sole discretion as to the method of making and publishing the Materials, including, without limitation, to all decisions regarding editing, lighting, filming, timing of publication, if any, length, quality, content and the like.

12. **Indemnification.** The Author agrees to indemnify JoVE and/or its successors and assigns from and against any and all claims, costs, and expenses, including attorney's fees, arising out of any breach of any warranty or other representations contained herein. The Author further agrees to indemnify and hold harmless JoVE from and against any and all claims, costs, and expenses, including attorney's fees, resulting from the breach by the Author of any representation or warranty contained herein or from allegations or instances of violation of intellectual property rights, damage to the Author's or the Author's institution's facilities, fraud, libel, defamation, research, equipment, experiments, property damage, personal injury, violations of institutional, laboratory, hospital, ethical, human and animal treatment, privacy or other rules, regulations, laws, procedures or guidelines, liabilities and other losses or damages related in any way to the submission of work to JoVE, making of videos by JoVE, or publication in JoVE or elsewhere by JoVE. The Author shall be responsible for, and shall hold JoVE harmless from, damages caused by lack of sterilization, lack of cleanliness or by contamination due to

the making of a video by JoVE its employees, agents or independent contractors. All sterilization, cleanliness or decontamination procedures shall be solely the responsibility of the Author and shall be undertaken at the Author's expense. All indemnifications provided herein shall include JoVE's attorney's fees and costs related to said losses or damages. Such indemnification and holding harmless shall include such losses or damages incurred by, or in connection with, acts or omissions of JoVE, its employees, agents or independent contractors.

13. **Fees.** To cover the cost incurred for publication, JoVE must receive payment before production and publication the Materials. Payment is due in 21 days of invoice. Should the Materials not be published due to an editorial or production decision, these funds will be returned to the Author. Withdrawal by the Author of any submitted Materials after final peer review approval will result in a US\$1,200 fee to cover pre-production expenses incurred by JoVE. If payment is not received by the completion of filming, production and publication of the Materials will be suspended until payment is received.

14. **Transfer, Governing Law.** This Agreement may be assigned by JoVE and shall inure to the benefits of any of JoVE's successors and assignees. This Agreement shall be governed and construed by the internal laws of the Commonwealth of Massachusetts without giving effect to any conflict of law provision thereunder. This Agreement may be executed in counterparts, each of which shall be deemed an original, but all of which together shall be deemed to be one and the same agreement. A signed copy of this Agreement delivered by facsimile, e-mail or other means of electronic transmission shall be deemed to have the same legal effect as delivery of an original signed copy of this Agreement.

A signed copy of this document must be sent with all new submissions. Only one Agreement is required per submission.

### CORRESPONDING AUTHOR

Name:

Sana Karam

Department:

Department of Radiation Oncology

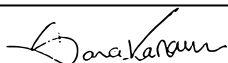
Institution:

University of Colorado Denver - Anschutz Medical Campus

Title:

Assistant Professor, Director of Radiobiology Research

Signature:



Date:

9/28/2018

Please submit a **signed** and **dated** copy of this license by one of the following three methods:

1. Upload an electronic version on the JoVE submission site
2. Fax the document to +1.866.381.2236
3. Mail the document to JoVE / Attn: JoVE Editorial / 1 Alewife Center #200 / Cambridge, MA 02140

## Response to Reviewers

### Reviewer #1:

Manuscript Summary:

This is a wonderful and interesting work. The idea is smart and the discussion is reasonable. The following weakness needs to be improved to enrich its value.

We appreciate the reviewer's positive feedback and recognition of the impact of this work.

Minor Concerns:

**1. As being mentioned that the size of tumors localized deep in the submucosa of buccal mucosa is measured by caliber, how authors can assure that the growth curve in Fig. 1B is accurate. This picture might need to be replaced by showing only the final volume or weight of the tumors yielded at the endpoints.**

This is an excellent point. While what the reviewer suggested is reasonable, we decided to take a more thorough and detailed approach at addressing this highly pertinent question. We conducted serial radiographic imaging with CT simultaneously with manual caliper measurement. The CT-based gross tumor volume was generated by contouring each and every section and volumetric measurements were assessed using ITK-SNAP Software. Tumor volume measurements were then correlated with caliper measurement and a correlation coefficient was obtained. These data are now shown in Figure 2C, which show excellent correlation  $R^2 = 0.8493$ . We further performed histological confirmation of the exophytic pattern of tumor growth and lack of tumor invasion into major neighboring structures such as the tongue, esophagus or bronchus. We added a sentence to clarify this point in the results section (shown below).

"Tumors did not invade into the tongue or other nearby organs (esophagus, bronchus, thymus) as assessed histologically."

**2. It is not sure whether the findings in Fig. 1 are owing to the discrepancy of in vitro or in vivo growth. Authors should provide the in vitro growth curve of both cell lines to signify their growth potential during cultivation.**

We thank the reviewer for highlighting this point. We have added the following sentence to our results section: "In vitro assessment of LY2 and B4B8 cell proliferation showed that both cell lines have similar doubling times (21 hours for LY2 and 23 hours for B4B8)."

**3. Scale bar of Fig. 2A should be provided as a reference for tumor size evaluation.**

A scale has been added.

**4. The description of (A) and (B) content in Fig. 3 should be detailed.**

A description has been added.

**5. To reorganize right panel of Fig. 3B is required. Myeloid cells and lymphoid cells should be shown in distinctive clusters.**

We have addressed this comment by splitting the graph into 2 graphs with myeloid and lymphoid cells presented separately (Figure 3C and Figure 3D).

**6. If possible, immune profile of B4B8 xenograft should be integrated in paper to compare with LY2 cells. This reviewer would think that the higher survival of B4B8 recipients may be associated with the stronger immunity. The comparison suggested would signify more the power of this study.**

We agree with the reviewer that adding flow cytometry data on B4B8 tumors may shed light on a different immune landscape in HNSCC. However, this is beyond the scope of this "methods" paper as dictated by the journal instructions. Immune profile data with these tumors has been published elsewhere (PMID: 30042205; PMID: 29123967). Our goal from this paper was to provide the scientific community detailed technique for inducing orthotopic HNSCC tumors. We hope that this has been achieved, especially after integrating reviewers' feedback.

### Reviewer #2:

Manuscript Summary:

This manuscript describes the development of a murine model system that is clinically- and physiologically-relevant to explore human head and neck squamous cell carcinoma. The authors use syngeneic and orthotopic murine cell



injection to the buccal mucosa which makes it relatively simple and easy to measure the tumor site, closely mimics human HNSCC, and has the advantage of an immunocompetent mice model system. The symptoms the mice demonstrated such as jaw displacement, and the histological and tumor microenvironment features show relevance to human head and neck squamous cell carcinoma.

Many thanks for the kind feedback.

Minor Concerns:

**1. The approved AICUC protocol details and number should be reported.**

We have included this information in the methods section of the manuscript:

"All animal procedures were performed in accordance with an approved institutional animal care and use committee (IACUC) protocol of the University of Colorado Denver (approval # 00250)."

**2. In page 3, section 15.1, RBC lysis buffer - the composition of the buffer should be described in detail.**

We added a description of the RBC lysis buffer in the appropriate section of the protocol:  
"RBC lysis buffer is comprised of ammonium chloride, sodium bicarbonate and disodium."

In addition, the specific product used is listed in the Jove excel file which is part of the manuscript.

**3. In page 3, section 15.4: HBSS the composition of buffer should be described in detail.**

We added a description of the RBC lysis buffer in the appropriate section of the protocol:  
"HBSS is comprised of HBSS is comprised of potassium chloride, sodium chloride, sodium bicarbonate, sodium phosphate dibasic, sodium phosphate monobasic and glucose."

In addition, the specific product used is listed in the Jove excel file which is part of the manuscript.

**4. Page 4 line 194: "tumor size" should be tumor volume.**

We thank the reviewer for highlighting this inadvertent mistake. We have corrected this.

**5. In the entire text, there should be a space left between the values and units, for example in section 14.1, "1-2mm" should be 1-2 mm, or in section 14.2, "50mL" should be 50 mL, etc.**

Our apologies. This too has been corrected.

*In compliance with data protection regulations, please contact the publication office if you would like to have your personal information removed from the database.*

**All editorial comments below have been addressed in the manuscript.**

**Editorial comments:**

1. Please take this opportunity to thoroughly proofread the manuscript to ensure that there are no spelling or grammar issues.

Done

2. Please provide an email address for each author.

Done

3. Keywords: Please provide at least 6 keywords or phrases.

Done

4. Please add a Long Abstract (150-300 words) before Introduction section. It should include a statement about the purpose of the method. A more detailed overview of the method and a summary of its advantages, limitations, and applications is appropriate. Please focus on the general types of results acquired.

Done

5. Please expand your Introduction to include the following: The advantages over alternative techniques with applicable references to previous studies; Description of the context of the technique in the wider body of literature; Information that can help readers to determine if the method is appropriate for their application.



[Done](#)

6. Please define all abbreviations before use.

[Done](#)

7. Please include an ethics statement before your numbered protocol steps, indicating that the protocol follows the animal care guidelines of your institution.

[Done](#)

8. Please add more details to your protocol steps. There should be enough detail in each step to supplement the actions seen in the video so that viewers can easily replicate the protocol. Please ensure you answer the “how” question, i.e., how is the step performed? Alternatively, add references to published material specifying how to perform the protocol action. See examples below.

[Done](#)

9. 2.1: How long does it take to reach 70% confluence?

10. 3.2: Please specify the reaction conditions (temperature and time).

11. 3.4: Resuspend cell in what media? Please specify. How is the cell number counted?

12. 6.1: Please specify the age, gender and strain of mice as well as the concentration of isoflurane.

13. 12: Please specify all surgical instruments used throughout the protocol.

14. 13.1: Please specify the concentration of formalin and the temperature.

15. 15.3: Please specify incubation temperature.

16. 17.1: What volume is considered to be appropriate?

17. 18: Please describe how to perform staining and analyze data.

[Done](#)

18. Please combine some of the shorter Protocol steps so that individual steps contain 2-3 actions and maximum of 4 sentences per step.

[Done](#)

19. Please include single-line spaces between all paragraphs, headings, steps, etc.

[Done](#)

20. After you have made all the recommended changes to your protocol (listed above), please highlight 2.75 pages or less of the Protocol (including headings and spacing) that identifies the essential steps of the protocol for the video, i.e., the steps that should be visualized to tell the most cohesive story of the Protocol.

[Done](#)

21. P

lease highlight complete sentences (not parts of sentences). Please ensure that the highlighted part of the step includes at least one action that is written in imperative tense. Please do not highlight any steps describing anesthetization and euthanasia.

[Done](#)

22. Please include all relevant details that are required to perform the step in the highlighting. For example: If step 2.5 is highlighted for filming and the details of how to perform the step are given in steps 2.5.1 and 2.5.2, then the sub-steps where the details are provided must be highlighted.

[Done](#)

23. Please remove the titles and Figure Legends from the uploaded figures. The information provided in the Figure Legends after the Representative Results is sufficient.

[Done](#)

24. Figures 1 and 2: Please include a space between the number and the units of the scale bar.

[Done](#)

25. Figure 3: Please explain both panels (A and B) in the figure legend. Please include a space between all numbers and their corresponding units (i.e., 5 mL, 50 mL, 37 °C, 70 µm). Please use the micro symbol µ instead of u. Please define error bars in the figure legend.

[Done](#)

26. Discussion: As we are a methods journal, please also discuss critical steps within the protocol, any modifications and troubleshooting of the technique, and any limitations of the technique.

[We have added the following sentences in the appropriate parts of the discussion:](#)

“Although, injection of cells into the buccal mucosa is straightforward, positioning of the needle and depth of penetration are critical to prevent puncture through the skin and ensure cells are not injected subcutaneously. We

recommend inserting the needle intra-orally while it is perfectly parallel to the buccal and tilting by no greater than 10 degrees when ready to inject.”

“To ensure maximum retrieval of viable single cells from tumors, use of digestion enzymes is necessary. Collagenase-based digestion enzymes can be harsh on cells and optimization of the concentration and type of collagenase maybe necessary for different tumor types. We compared 5 digestion enzymes before determining that Collagenase III which was used in this study is the optimal method for digestion of squamous cell tumors.”

27. For in-text references, the corresponding reference numbers should appear as superscripts after the appropriate statement(s) in the text (before punctuation but after closed parenthesis). The references should be numbered in order of appearance.

[Done](#)

28. Please ensure that the references appear as the following: [Lastname, F.I., LastName, F.I., LastName, F.I. Article Title. Source. Volume (Issue), FirstPage – LastPage (YEAR).] For more than 6 authors, list only the first author then et al. See the example below:

Bedford, C.D., Harris, R.N., Howd, R.A., Goff, D.A., Koolpe, G.A. Quaternary salts of 2-[(hydroxyimino)methyl]imidazole. Journal of Medicinal Chemistry. 32 (2), 493-503 (1998).

[Done](#)

29. References: Please do not abbreviate journal titles.

The Jove Endnote reference style was downloaded and applied and yet journal titles were abbreviated in this file. If you have an endnote compatible file, we can use that instead.

30. Table of Equipment and Materials: Please revise the table of the essential supplies, reagents, and equipment to include the name, company, and catalog number of all relevant materials in separate columns in an xls/xlsx file. Please sort the items in alphabetical order according to the Name of Material/ Equipment.

[Done](#)